

# Miscible blends from rigid poly(vinyl chloride) and epoxidized natural rubber

## Part 1 Phase morphology

K. T. VARUGHESE, G. B. NANDO, P. P. DE, S. K. DE

Rubber Technology Centre, Indian Institute of Technology, Kharagpur 721 302, India

Miscible blends of rigid poly(vinyl chloride), PVC, and epoxidized natural rubber (ENR) having 50 mol% epoxidation level, are prepared in a Brabender Plasticorder by the melt-mixing technique. Changes in Brabender torque and temperature, density, dynamic mechanical properties and DSC thermograms of the samples are studied as a function of blend composition. The PVC-ENR blends behave as a compatible system as is evident from the single  $T_g$  observed both in dynamic mechanical analysis (DMA) and differential scanning calorimetry (DSC). The moderate level broadening of the  $T_g$  zone in blends is due to microinhomogeneity, which may arise from the particle structures of PVC perturbing the molecular level mixing of PVC and ENR. Scanning electron microscopic studies were conducted on nitric acid-etched samples and the results showed continuous structures of blend components as well as the occurrence of solvent-induced cracks in high PVC blends.

### 1. Introduction

Miscible polymer-polymer blends obtained from two components have a single-phase morphology corresponding to a single glass-rubber transition temperature ( $T_g$ ) lying between the two. The basis of this miscibility may arise from any specific interactions such as hydrogen bonding [1-6], dipole-dipole forces [7] and charge transfer complexes [8, 9] for homopolymer mixtures or segment-segment repulsion occurring inside a copolymer for copolymer-based blends [10-13]. Among the different blends capable of exhibiting a single-phase morphology are those based on PVC systems in which the specific interaction is suggested to be hydrogen bonding [1, 6].

The phase morphology of polyblends can be detected by dynamic mechanical analysis (DMA), differential scanning calorimetry (DSC) and scanning electron microscopy (SEM) of blends of different compositions. Blends are generally prepared by the techniques of solution casting or melt mixing. For compatible blends, both these methods may give single glass-rubber transition temperature ( $T_g$ ). However, two major drawbacks of solution-cast blends are (a) a greater lowering of  $T_g$  than the melt blends [14], and (b) the great dependence of polymer-polymer compatibility on the solvent used for casting [15]. For practical applications, melt blending is preferred, because this technique is industrially adaptable to obtain solvent-free and less expensive products of thermoplastic-thermoplastic or thermoplastic-rubber blends.

Recent studies on polyblends have shown that PVC has a great affinity towards epoxidized natural rubber especially when the epoxidation level is about 50 mol% [16-18]. Epoxidized natural rubber (ENR) is prepared at the latex stage by the partial and random oxidation

of natural rubber with a peracid [19, 20]. Baker *et al.* [21, 22] have reported that the 50 mol% ENR exhibits strain-induced crystallization as in natural rubber, an oil resistance similar to medium acrylonitrile rubber, high damping, good wet grip characteristics and low rolling resistance. Margaritis and Kalfoglou [17] have reported that 50 and 25 mol% ENR form miscible and partially miscible blends, respectively, with PVC when mixed in solution. In addition, the use of epoxidized oils as a secondary plasticizer in PVC is well known. Recently, Feldman *et al.* [23] have studied the morphology of epoxy polymer-PVC blends and reported that the system is immiscible at lower concentrations of the second component (up to 10%), but they become mutually and increasingly miscible as the concentration of PVC becomes higher. Our earlier studies, based on melt blends [18], have shown that 50 mol% epoxidized natural rubber (ENR) is capable of functioning as a polymeric plasticizer depressing the melt viscosity of rigid PVC. Encouraged by this observation and considering the novelty and importance of the system as a probable commercial material in the near future, we have undertaken the present investigation on phase morphology of rigid PVC-ENR blends.

### 2. Experimental procedure

Details of the materials used and the formulation of the mixes are given in Tables I and II, respectively. The mixes are denoted P<sub>100</sub>, P<sub>70</sub>, P<sub>50</sub>, P<sub>30</sub> and P<sub>0</sub>, corresponding to the weight percentage of PVC in the blends.

Prior to blending of PVC with ENR, the powdered PVC resin was initially mixed with 6 p.h.r. of the stabilizer, tribasic lead sulphate (TBLS) in a Brabender

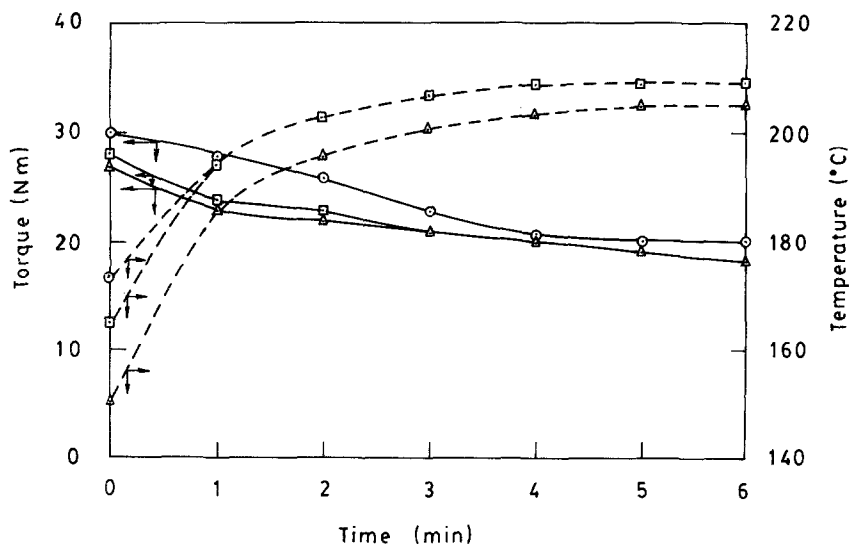


Figure 1 Effect of mixing time on the Brabender torque and temperature of PVC-ENR blends. (○) P<sub>70</sub>, (□) P<sub>50</sub>, (△) P<sub>30</sub>.

Plasticorder (model PLE 330) using a cam-type mixer at a rotor speed of 100 r.p.m. and temperature of 110°C for 15 min.

The blending of PVC resin with ENR was performed at 180°C maintaining the rotor speed at 60 r.p.m. in the Brabender Plasticorder. Torque and temperature developed were recorded. At the start, PVC resin was allowed to melt for 2 min and ENR was added thereafter. The total mixing time of ENR with molten PVC was 6 min in all cases. The molten mix was then quickly removed from the chamber and sheeted out in the tight nip of a laboratory two-roll mill. The sheeted-out stock was compression moulded at 180°C for 3 min. The hot mould with the blended material inside was then quenched in a stream of cold water for 1 min before taking the sample out. The densities of all the samples were measured.

Dynamic mechanical properties were measured using a Rheovibron DDV III-C at a strain amplitude of 0.0025 cm and a frequency of 3.5 Hz. The general procedure was to cool the sample to -100°C and record the measurements during the warm-up. The temperature rise was 1°C min<sup>-1</sup>.

DSC experiments were run on a DuPont thermal analyser model 910, in a nitrogen atmosphere.  $T_g$ s of

the samples were taken as the mid-point of the step in the scan, run at a heating rate of 20°C min<sup>-1</sup>.

In order to study the phase structure using SEM, the cryogenically fractured blends were etched with concentrated nitric acid at 50°C for 50 h to remove the ENR phase. The reacted nitric acid was frequently removed and replaced with fresh acid. The samples were washed and dried, and SEM measurements were made on Philips 500 model scanning electron microscope at a tilt angle of 33°.

### 3. Results and discussion

#### 3.1. Brabender torque and stock temperature

Mixing parameters which could influence the phase morphology and final strength properties of the Brabender-mixed products are rotor speed, temperature, mixing time and the total volume of the mixing components. Maintaining these parameters constant, the torque and stock temperature up to 6 min mixing were noted and their plots in terms of blend composition are given in Fig. 1. It is seen that the addition of ENR into rigid PVC reduces the torque as a result of lowering of the melt viscosity in the blends. This feature can be attributed to the plasticization of rigid PVC by ENR as reported in earlier studies [18]. P<sub>70</sub> attains a final steady torque at the fifth minute of mixing, whereas P<sub>50</sub> and P<sub>30</sub> tend to have a slow decrease without maintaining a steady torque. The absence of a final steady torque in P<sub>50</sub> and P<sub>30</sub> indicates their time-dependent shear degradative action. The prolonged shearing may enhance chain scission in ENR and reduce the melt viscosity, which in turn lowers the torque in the blends.

Stock temperatures measured during the mixing of different compositions are plotted in Fig. 1. The observed initial lower value of stock temperature than the mixing temperature (180°C) for blends is due to

TABLE I Details of materials used

Materials	Characteristics/ literature data	Source
Poly(vinyl chloride), (PVC)	Suspension-polymerized PVC (NOCIL PVC Polymer S67-311)K value 66 to 69	NOCIL, Bombay
Tribasic lead sulphate (TBLS)	Lead-based stabilizer for PVC	Waldies Ltd, Calcutta
Epoxidized natural rubber (ENR)	50 mol % epoxidized natural rubber. Mooney viscosity ML <sub>(1+4)</sub> 100°C, 140, specific gravity 1.03, glass transition temperature -20 ± 2°C	The Malaysian Rubber Producers Research Association, Brickendonbury, UK

TABLE II Formulations of rigid PVC-ENR blends

	Blend code				
	P <sub>100</sub>	P <sub>70</sub>	P <sub>50</sub>	P <sub>30</sub>	P <sub>0</sub>
Rigid PVC (wt %)	100	70	50	30	0
ENR (wt %)	0	30	50	70	100

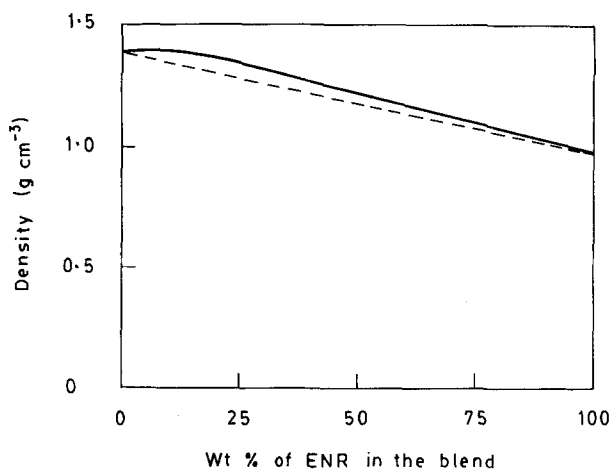


Figure 2 Density changes of PVC-ENR blends.

the depression in temperature on adding ENR to the molten PVC. However, the vigorous mixing causes a steep rise of the stock temperature even in the first minute of blending. As the blending progresses, the stock temperature undergoes a gradual rise until a final steady temperature is attained. The curves of  $P_{70}$  and  $P_{50}$  merge and attain a final steady temperature at the fourth minute of mixing.  $P_{30}$  maintains a final steady temperature which is slightly lower than that of

TABLE III Density,  $T_g$ , and width of  $T_g$  zone in PVC-ENR blends

Samples	Density ( $\text{g cm}^{-3}$ )	$T_g$ ( $^{\circ}\text{C}$ )			Width of $T_g$ (DSC) zone, $\Delta T$ ( $^{\circ}\text{C}$ )
		$E''$	Tan $\delta$	DSC	
$P_{100}$	1.390	85.0	92.0	84.0	11.0
$P_{70}$	1.315	36.0	57.0	28.0	34.0
$P_{50}$	1.215	14.0	29.0	17.0	19.0
$P_{30}$	1.116	-1.0	11.0	-7.5	14.0
$P_0$	0.982	-8.0	-1.0	-17.0	11.0

$P_{70}$  and  $P_{50}$  at the fifth minute of mixing. The observed increase in temperature ( $\Delta T$ ) during mixing has been found to be 29, 29 and 25 $^{\circ}\text{C}$  corresponding to  $P_{70}$ ,  $P_{50}$  and  $P_{30}$ , respectively. The attainment of final steady temperature indicates a uniform exothermic mixing in PVC-ENR blends. In summary, the torque and temperature values of all blends indicate a satisfactory level of mixing of PVC and ENR at the end of 6 min mixing time in the Brabender Plasticorder.

### 3.2. Density

Experimental values of density of all samples are shown in Table III. It has been found that the

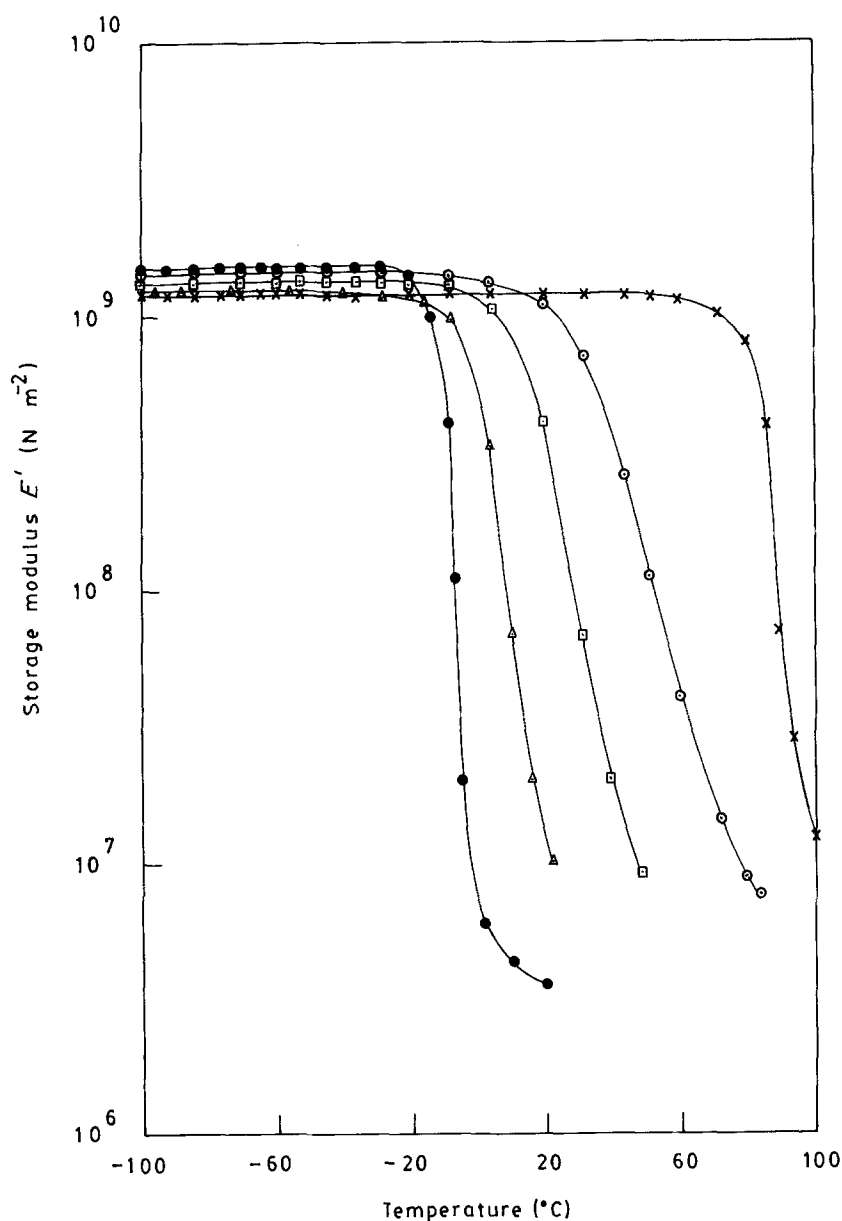


Figure 3 Effect of temperature on storage modulus of PVC-ENR blends. (x)  $P_{100}$ , (o)  $P_{70}$ , (□)  $P_{50}$ , (Δ)  $P_{30}$ , (●)  $P_0$ .

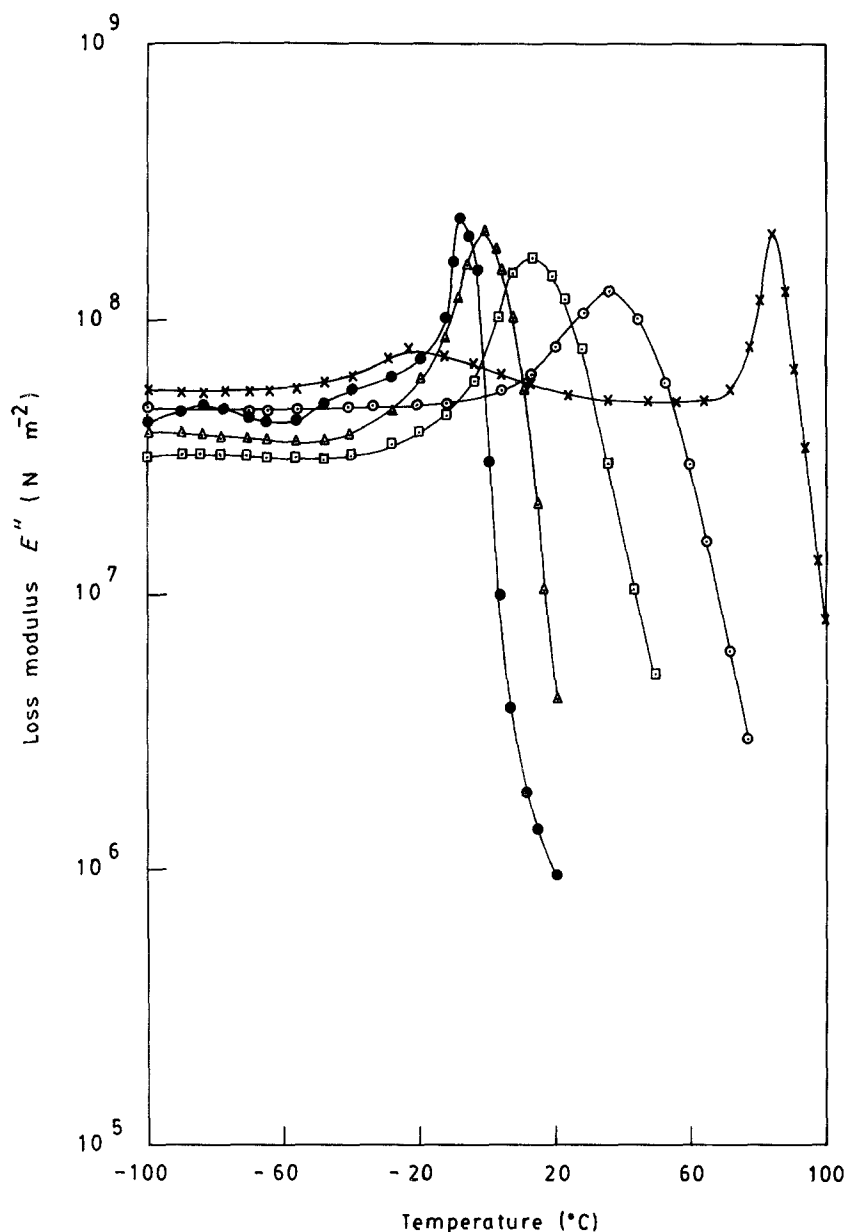


Figure 4 Effect of temperature on loss modulus of PVC-ENR blends. (x) P<sub>100</sub>, (o) P<sub>70</sub>, (□) P<sub>50</sub>, (Δ) P<sub>30</sub>, (●) P<sub>0</sub>.

experimental values of blends lie above the calculated values (Fig. 2). This phenomenon could be understood in terms of packing densification in PVC-ENR blends. A similar nature of density dependence of blend composition has also been reported by Zakrezewski [24] for miscible NBR-PVC systems.

### 3.3. Dynamic mechanical properties

Dynamic storage modulus ( $E'$ ), loss modulus ( $E''$ ) and damping ( $\tan \delta$ ) of different compositions are shown in Figs 3 to 5. Pure PVC and ENR exhibit both  $\alpha$ -relaxation corresponding to  $T_g$ , and secondary transition of the glassy state, whereas blends have only  $\alpha$ -transition. The small broad transition for PVC at  $-26^\circ\text{C}$  is the  $\beta$ -transition occurring from the local segmental motions of the main chain. Minor transitions for ENR at  $-45$  and  $-82^\circ\text{C}$  in the glassy region may be the result of any structural defect in the material. In blends, however, the secondary transitions are not evident. Suppression of the secondary relaxations due to the interaction of blend components has been reported earlier [25, 26].

For all compositions, blends show a single  $T_g$ .

Dynamic storage modulus rapidly decreases at the  $T_g$  zone, due to the decrease in stiffness of the samples. Concomitantly, loss modulus and damping sharply increase until they attain their maxima and then fall with increasing temperature. The temperature corresponding to the maxima in damping or loss modulus is chosen as the  $T_g$  of the polymer (Table III). As a general trend in polymer systems, the temperature corresponding to the loss modulus maximum, in all cases, is found to be lower than that of the damping maximum. From Figs 4 and 5, it is quite evident that the blends have only one  $T_g$ , which occurs in between the  $T_g$ s of the individual components. This indicates that the system is compatible at all compositions. However, a detailed examination of the results of dynamic mechanical analysis (DMA) reveals broadening of the glass-rubber transition zone of blends, particularly, in high PVC systems. This aspect will be discussed later while discussing the results of thermal analysis. The loss modulus and the damping maxima of blends appear to lie below that of the pure components as a result of the specific interaction existing between the rigid PVC and ENR.

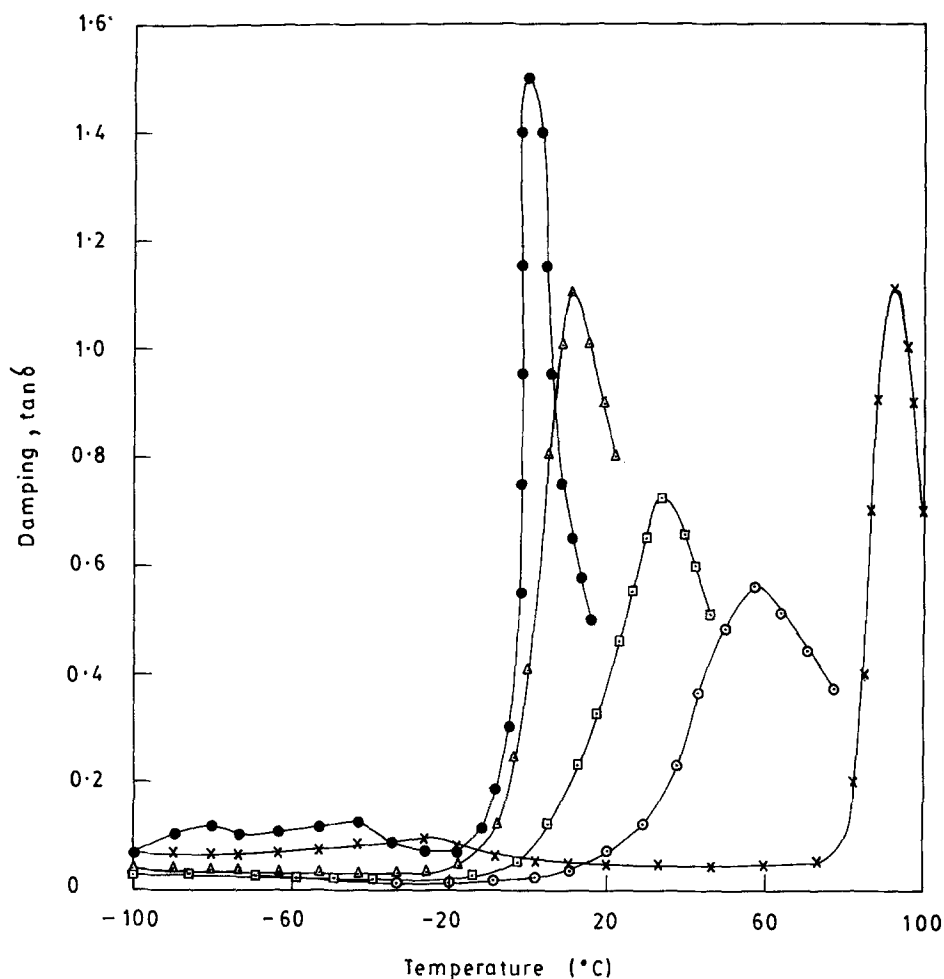


Figure 5 Effect of temperature on damping ( $\tan \delta$ ) of PVC-ENR blends. (x) P<sub>100</sub>, (O) P<sub>70</sub>, (□) P<sub>50</sub>, (Δ) P<sub>30</sub>, (●) P<sub>0</sub>.

### 3.4. DSC thermograms

Additional evidence for the mutual solubility of rigid PVC and ENR is supported by the DSC thermograms as shown in Fig. 6. Blends exhibit a single  $T_g$ , which is progressively shifted to lower temperatures as the ENR content increases. As observed in the case of DMA results, the glass-rubber transition zone becomes broadened in blends. The magnitude of this broadening and the transition width temperature ( $\Delta T$ ) has been measured and is shown in Fig. 7 and Table III. P<sub>70</sub> shows the maximum broadening and a transition width temperature of 34°C. In contrast to the DMA results, DSC thermograms of blends at lower temperature exhibit irregular secondary transitions, which are more pronounced for P<sub>70</sub> and P<sub>30</sub>. Moreover, the  $\beta$ -transition in PVC is not prominent, and for ENR, instead of the minor transitions at -45 and -82°C as observed in DMA, a small single transition at -76°C is observed in the DSC results. This indicates quite a different nature of response in molecular segments of the samples towards dynamic mechanical analysis and differential scanning calorimetric analysis conditions. However, the segmental motion of molecular chains at the glassy zone is less important than the glass-rubber transition zone in predicting the phase morphology of polyblends.

### 3.5. Broad $T_g$ transition in PVC-ENR blends

The behaviour of  $\alpha$ -relaxation (transition) in DMA and in DSC confirms no phase separation in the

blends. However, the probability of any microlevel inhomogeneity, as may be visualized from the broad  $T_g$  transitions in blends, is not ruled out. A gross level broadening or increase in the width of transition in blends may be considered as a tendency to undergo phase separation of blend components. For instance, phase separation of blend components for certain compositions has been reported by Schurer *et al.* [27] for poly(methyl methacrylate)/poly(vinyl chloride) systems, and by Vukovic *et al.* [28] for poly(2,6 dimethyl 1,4 phenylene oxide)/poly(fluorostyrene-co-chlorostyrene) systems. A minor or moderate level of such broadening in blends is generally recognized as an indication of microheterogeneity. In PVC-ENR systems, while PVC and ENR have an almost equal width of  $T_g$  transition, it becomes progressively broadened as the content of PVC is increased. This is due to minor inhomogeneity in the blends of PVC and ENR. The  $T_g$  transition width temperature ( $\Delta T$ ) measured from DSC thermograms as plotted against blend composition, is shown in Fig. 7. The maximum for the 70 wt % PVC indicates that there is an optimum composition of blend components, where the broadening reaches a maximum. We attribute this inhomogeneity in terms of particulate structures or molecular aggregates bound by crystallites of PVC [29-33]. These structures perturb the molecular level mixing of ENR with PVC despite the high interaction between them. A scanning electron micrograph showing partially fused aggregated particle structures of PVC in

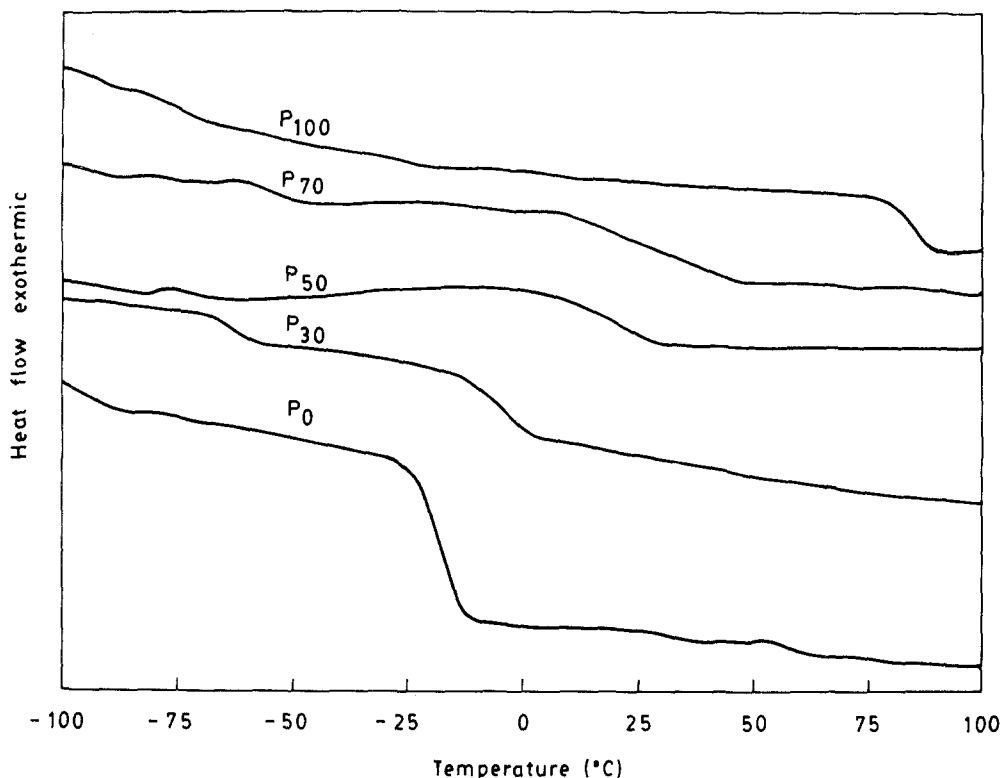


Figure 6 DSC thermograms of PVC-ENR blends.

our study is given in a subsequent paper [34]. The perturbation is more affected in P<sub>70</sub> because the minor component ENR is incapable of disrupting PVC aggregates and interacting with the molecules inside. The higher level of ENR, however, causes a dilution effect and hence disruption of these aggregated structures by ENR. Disruption of these microdomains of PVC may also be achieved by longer milling time and higher processing temperature. In plasticized PVC systems, Soni *et al.* [35] observed inhomogeneous distribution of plasticizers such as dioctyl phthalate, nitrile rubber and ethylene vinyl acetate copolymer due to the presence of unplasticized microdomains of PVC. Hence, a certain level of inhomogeneity as indicated by the broadening of glass-rubber transition may be expected even in miscible systems of PVC-ENR.

### 3.6. Concavity in the $T_g$ -composition curve

Effect of blend ratio on  $T_g$  values (Table III) obtained from the maxima in loss modulus and damping, and DSC thermograms is shown in Fig. 8.  $T_g$  obtained from the damping ( $\tan \delta$ ) maximum is found to be much higher than that of the loss modulus maximum and DSC thermograms. In each case, the results have been tested with the commonly used Fox relationship [36],

$$1/T_{gb} = W_1/T_{g1} + W_2/T_{g2} \quad (1)$$

where,  $T_{gb}$ ,  $T_{g1}$  and  $T_{g2}$  are the glass-rubber transition temperatures of blend, component 1 and component 2, respectively, and  $W_1$  and  $W_2$  are the weight fractions of the components 1 and 2, respectively. The experimental values obtained by the three different methods are different and again each is less than that of the

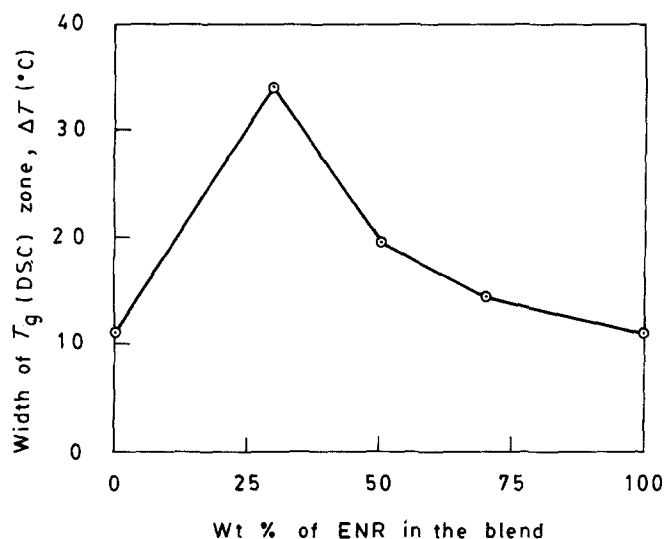


Figure 7 Effect of blend ratio on width of  $T_g$  (DSC) zone in PVC-ENR blends.

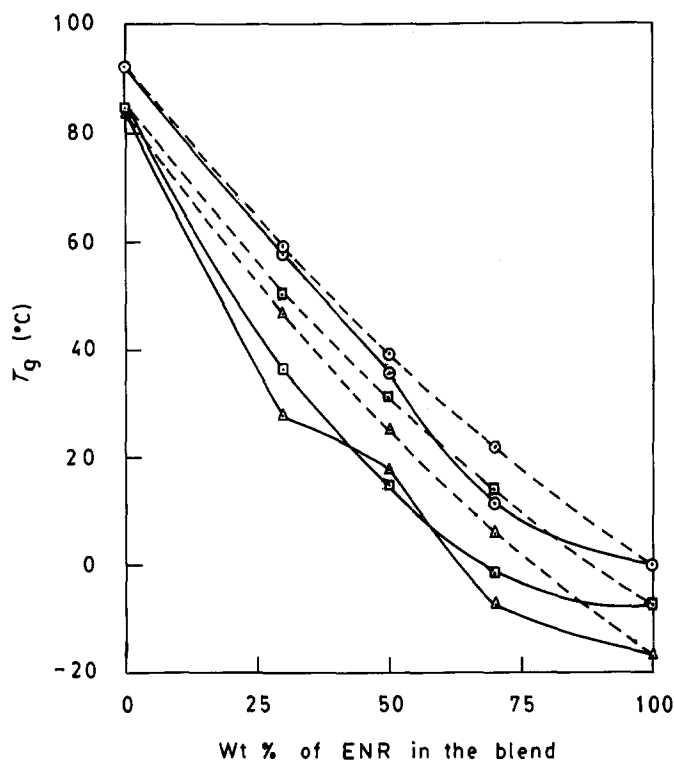


Figure 8 Effect of blend ratio on  $T_g$  of PVC-ENR blends. (●)  $\tan \delta$  values, (□)  $E''$  values, (△) DSC values, (---) Fox relationship.

calculated values based on Equation 1. The  $T_g$  ( $\tan \delta$ )-composition curve appears to have a closer agreement with the Fox relationship than the  $T_g$  ( $E''$ )-composition and  $T_g$  (DSC)-composition curves. A salient feature of Fig. 8 is the concavity of the curves, particularly at the mid-composition region. Similar concavity has been recognized as a common feature in miscible systems of polymer-plasticizer [37-39] and polymer-polymer [40, 41]. The existence of cusp or concavity in PVC-plasticizer and blends between low molecular weight substances has been tentatively attributed by Scandola and co-workers [37, 38] to the occurrence of some morphological transition at a critical diluent concentration. Roy and co-workers [39, 40] attributed such a phenomenon to the contribution of the excess volume of mixing to the free volume.

### 3.7. Scanning electron micrographs

In order to observe the microstructure of the phase of a binary component system using SEM, generally, one of the components is removed by selective etching with a suitable solvent. In our studies, among several sol-

vents tried, we found that the ENR portion in blends could be satisfactorily etched by nitric acid. The use of nitric acid for etching the elastomeric component in blends has also been reported by Ito *et al.* [42] and Akhtar *et al.* [43]. Scanning electron micrographs of nitric acid etched blends of PVC-ENR are shown in Figs 9 to 11. Interestingly,  $P_{70}$  and  $P_{50}$ , in addition to the continuous phase structure of the components, exhibit solvent-induced cracks developed from solvent-induced crazes [44]. Macrolevel domain structure of ENR is not seen in any of the micrographs. This gives an impression of the continuous structure of PVC and ENR in blends. Some tiny holes, however, present particularly in the micrographs of  $P_{70}$  and  $P_{50}$ , are due to the microdomains of ENR. As the content of ENR in blends increases, the micrographs show more distinct elongated structures of the components. These results suggest that during the process of mixing, ENR and PVC chains associate and intermingle through forces of specific interaction, which can overcome the cohesive forces existing among the molecules in each of the blend components.

Cracks seen in  $P_{70}$  and  $P_{50}$  are the opened up

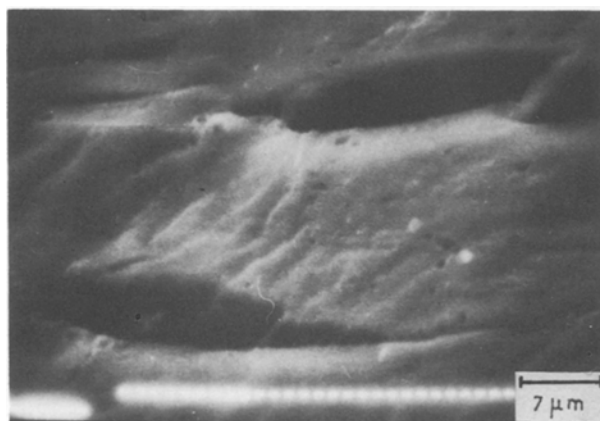


Figure 9 SEM of nitric acid-etched  $P_{70}$ .

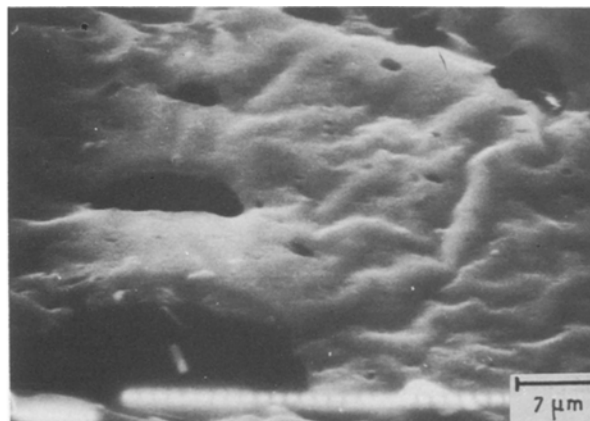


Figure 10 SEM of nitric acid-etched  $P_{50}$ .

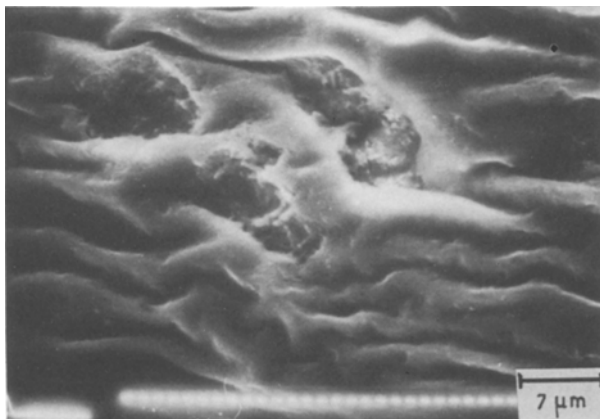


Figure 11 SEM of nitric acid-etched  $P_{30}$ .

solvent-induced crazes [44]. Remnant craze fibrils are quite evident inside the cracks in the micrograph of  $P_{70}$ . Crazed cracks in  $P_{70}$  are long and narrow, whereas that in  $P_{30}$  are short and broad. In the case of  $P_{30}$ , no cracks appear due to crazes. In high PVC compositions, the strongly bonded PVC-ENR segments prevent the acid from selectively etching ENR. However, the corrosion continues and localized stresses develop. As a result, several craze fibrils grow at the stress concentrated regions and eventually open up into several large cracks. In low PVC compositions, nitric acid overcomes the force of interaction between the blend components and so ENR is easily removed. Moreover, the high proportion of ENR in blends enables the developing stress to be dissipated homogeneously throughout the matrix and avoid crazing and cracking.

#### 4. Conclusions

From the above discussions and analysis, it is concluded that melt-mixed blends of rigid PVC and ENR (epoxidation level, 50 mol %) have a phase morphology close to a single-phase system. These blends have a single  $T_g$  lying between the  $T_g$ s of the pure components as is evident from dynamic mechanical analysis and DSC thermograms. Moderate level broadening or increase in the width of the glass-rubber transition temperature occurs with increasing PVC concentration in the blends. This microinhomogeneity is due to the particle structure of PVC perturbing the mutual solubility of PVC and ENR at molecular level. As a general trend of miscible systems, the  $T_g$ -blend composition curve is concave at the mid-composition region of PVC-ENR blends. Scanning electron micrographs of nitric acid-etched blends reveal the elongated phase structure of PVC and ENR as well as solvent-induced cracks in high PVC compositions. Specific interaction occurring between the polar groups of PVC and ENR help in mixing and forming a single phase in the blends.

#### Acknowledgements

One of the authors (KTV) thanks Professor S. K. Sanyal, Department of Chemical Engineering, Jadavpur University, Jadavpur, for helpful suggestions and the Department of Science and Technology, New Delhi, for sponsoring the project.

#### References

- O. OLABISI, *Macromol.* **8** (1975) 316.
- S. DJADOUN, R. N. GOLDBERG and H. MORAWETZ, *ibid.* **10** (1977) 1015.
- S. P. TING, B. J. BULKIN, E. M. PEARCE and T. K. KWEI, *J. Polym. Sci. Polym. Chem. Edn* **19** (1981) 1451.
- J. LECOURTIER, F. LAFUMA and C. Y. P. QUIVORON, *Makromol. Chem.* **183** (1982) 2021.
- R. STADLER and J. BURGERT, *ibid.* **187** (1986) 1681.
- E. BENEDETTI, A. DALESSIO, M. AGLIETTO, G. RUGGERI, P. VERGAMINI and F. CIARDELLI, *Polym. Engng Sci.* **26** (1986) 9.
- M. AUBIN, Y. BEDARD, M. F. MORRISSETTE, R. E. PRUD'HOMME, *J. Polym. Sci. Polym. Phys. Edn* **21** (1983) 233.
- T. SULZBERG and R. J. COTTER, *J. Polym. Sci. Part A-1* **8** (1970) 2747.
- N. OHNO and J. KUMANOTANI, *Polym. J.* **11** (1979) 947.
- R. P. KAMBOUR, J. T. BENDLER and R. C. BOPP, *Macromol.* **16** (1983) 753.
- G. TEN BRINKE, F. E. KARASZ and W. J. MACKNIGHT, *ibid.* **16** (1983) 1827.
- D. R. PAUL and J. W. BARLOW, *Polymer* **25** (1984) 487.
- T. SHIOMI, F. E. KARASZ and W. J. MACKNIGHT, *Macromol.* **19** (1986) 2274.
- T. NISHI, T. K. KWEI and T. T. WANG, *J. Appl. Phys.* **46** (1975) 4157.
- M. BANK, J. LEFFINGWELL and C. THIES, *Macromol.* **4** (1971) 43.
- I. R. GELLING, *NR Technol.* **16** (1985) 1.
- A. G. MARGARITIS and N. K. KALFOGLOU, *Polymer* **28** (1987) 497.
- K. T. VARUGHESE, P. P. DE, G. B. NANDO and S. K. DE, *J. Vinyl Technol.* **9** (4) (1987) 160.
- I. R. GELLING, *Rubb. Chem. Technol.* **58** (1985) 86.
- S. C. NG and L. H. GAN, *Eur. Polym. J.* **17** (1981) 1073.
- C. S. L. BAKER, I. R. GELLING and R. NEWELL, *Rubber Chem. Technol.* **58** (1985) 67.
- C. S. L. BAKER, I. R. GELLING and A. B. SAM-SURI, *J. Nat. Rubber Res.* **1** (1986) 135.
- D. FELDMAN, A. BLAGA and E. CORIATY, *J. Appl. Polym. Sci.* **29** (1984) 515.
- G. A. ZAKRZEWSKI, *Polymer* **14** (1973) 347.
- J. V. KOLESKE and R. D. LUNDBERG, *J. Polym. Sci. Polym. Phys. Edn* **7** (1969) 795.
- J. J. HICKMAN and R. M. IKEDA, *ibid.* **11** (1973) 1713.
- J. W. SCHURER, A. DeBOER and G. CHALLA, *Polymer* **16** (1975) 201.
- R. VUKOVIC, V. KURESEVIC, N. SEGUDOVIC, F. E. KARASZ and W. J. MACKNIGHT, *J. Appl. Polym. Sci.* **28** (1983) 1379.
- A. R. BERENS and V. L. FOLTS, *Trans. Soc. Rheol.* **11** (1967) 95.
- H. T. KAUF and F. E. FILISKO, *Macromol.* **12** (1979) 479.
- J. ELIASSEF, *J. Macromol. Sci. Chem.* **A8** (1974) 459.
- J. A. DAVIDSON and D. E. WITTENHAFFER, *J. Polym. Sci. Polym. Phys. Edn* **18** (1980) 51.
- P. H. GEIL, *J. Macromol. Sci. Phys.* **B14** (1977) 171.
- K. T. VARUGHESE, P. P. DE and S. K. SANYAL, *J. Mater. Sci.* **23** (1988) in print.
- P. L. SONI, P. H. GEIL and E. A. COLLINS, *J. Macromol. Sci. Phys.* **B20** (1981) 479.
- T. G. FOX, *Bull. Amer. Phys. Soc.* **1** (1956) 123.
- M. SCANDOLA, G. GECORULLI, M. PIZZOLI and G. PEZZIN, *Polym. Bull.* **6** (1982) 653.
- M. PIZZOLI, M. SCANDOLA, G. GECORULLI and G. PEZZIN, *ibid.* **9** (1983) 429.
- S. K. ROY, G. R. BROWN and St. PIERRE, *Int. J. Polym. Mater.* **10** (1983) 13.
- A. K. NANDI, B. M. MANDAL, S. N. BHATTA-



- CHARYYA and S. K. ROY, *Polym. Commun.* **27** (1986) 151.
41. G. BELORGY and R. E. PRUD'HOMME, *J. Polym. Sci. Polym. Phys. Edn* **20** (1982) 191.
42. J. ITO, K. MITANI and Y. MIZUTANI, *J. Appl. Polym. Sci.* **30** (1985) 497.
43. S. AKHTAR, B. KURIAKOSE, P. P. DE and S. K. DE, *Plast. Rubb. Process. Appl.* **7** (1987) 11.
44. J. I. KROSCWITZ (ed.), "Encyclopedia of Polymer Science and Engineering", Vol. 4 (Wiley, New York, 1986) p. 318.

*Received 5 November 1987  
and accepted 1 March 1988*